

WIDEBAND SHORTED ANNULAR STACKED PATCH ANTENNA FOR GLOBAL NAVIGATION SATELLITE SYSTEM APPLICATION WITH COMPACT SIZE AND BROAD BEAMWIDTH CHARACTERISTICS

Xi Li*, Lin Yang, Min Wang, Yi Wang, Xi Chen, and Juan Lei

National Laboratory of Science and Technology on Antennas and Microwaves, Xidian University, Xi'an, Shaanxi, China

Abstract—A compact circularly polarized shorted annular stacked patch antenna has been proposed for global navigation satellite system (GNSS) in this paper. The antenna has been designed to operate for the satellite navigation frequencies including GPS, GLONASS, Galileo and Compass (1100 MHz–1600 MHz). In order to obtain wideband characteristics, broadband 90° hybrids have been used as a secondary network. The designed antenna has a 73.7% (10-dB) return loss bandwidth from 0.9 GHz to 1.95 GHz, and 60.1% 3-dB axial ratio bandwidth from 0.96 GHz to 1.8 GHz, respectively. Shorted annular stacked patch structure is incorporated into the antenna design helping to obtain stable gain bandwidth, broad beamwidth characteristics and good axial ratio at low elevation. The designed antenna occupies a compact size of 100 mm × 100 mm × 15.5 mm.

1. INTRODUCTION

With the development of global navigation satellite system (GNSS), the requests for multi-system navigation ability increase. To fulfill the needs of this application, antennas should be wideband, with stable gain bandwidth, broad beamwidth and compact size. Quadrifilar helical antenna has exciting radiation characteristics of broad beamwidth [1,2]. However, the disadvantages of big size and narrow bandwidth limit its applications. Microstrip patch antennas [3–6,8–11,13–21] are often used in the applications needing circular polarization due to their low-profile, low cost, easy fabrication and

Received 19 October 2012, Accepted 12 December 2012, Scheduled 13 December 2012

* Corresponding author: Xi Li (xli@xidian.edu.cn).

compatibility with integrated circuit technology. However, the general limitations of the traditional microstrip antennas are achievable impedance and axial-ratio (AR) bandwidths. There are many methods to achieve broadband performance of microstrip antennas, such as using two or more radiating structures which work at different but contiguous resonant frequencies, using coupling feeding scheme, adding external matching circuits and so on. Several multi-band or wideband low-profile antennas have been proposed in the literature [7–11] for GPS or GNSS application. However, few of them can obtain broad beamwidth characteristics and good axial ratio at low elevation, which are useful to suppressing multipath interferences.

In this paper, a novel proximity-coupled probe-fed shorted annular stacked patch antenna design for GNSS application has been presented, which can be used in all four satellite navigation services. The presented antenna is characterized by the following features: 1) in order to obtain wideband impedance and AR bandwidths, broadband 90° hybrids and printed L-probes coupling feeding schemes are used. 2) The ground plane and feeding network are printed on the lower and higher side of the substrate respectively. In this case, the network can be fed by an SMA connector from the bottom of substrate, which is propitious to feeding the array. This structure can also make the antenna symmetrical and have a symmetrical radiation performance. 3) The feeding network is arranged along the diagonal of the substrate, helping to optimize the space utilization. 4) The usage of shorted annular stacked patch as radiator instead of conventional patch, which can provide stable gain bandwidth, broad beamwidth characteristics and good axial ratio at low elevation.

In Section 2, the antenna configuration and design principle are described. The simulated and measured antenna parameters are given in Section 3, followed by a brief conclusion in Section 4.

2. ANTENNA CONFIGURATION AND DESIGN

Figure 1 presents the structure of the proposed shorted annular stacked patch antenna. The antenna design includes five layers. The upper annular patch is printed on the top of the first substrate layer and the lower annular patch printed on the back. The upper and lower patches are shorted by the metal wall. The second substrate layer acts as the support and isolates the lower patch and L-probe. The L-probes are proposed to achieve broadband matching. In this design, four L-probes are placed under the radiating patch to excite the annular ring and transform the input impedance. The L-probes are composed of four square metal strips, printed on the top of the third substrate and

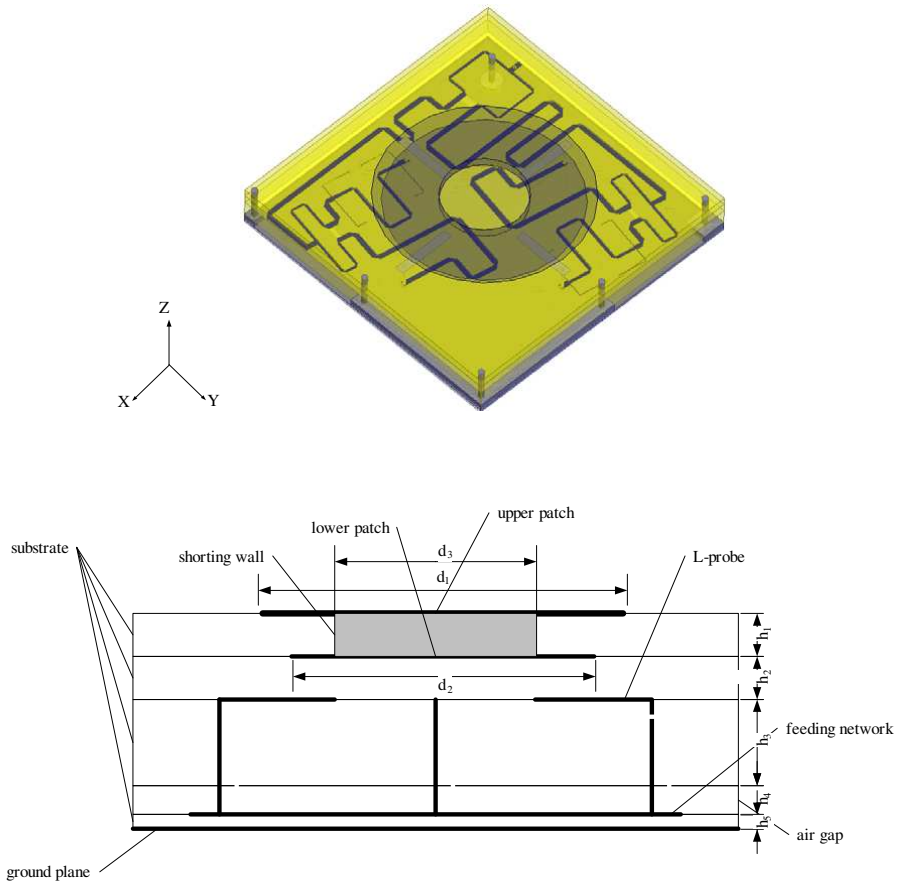


Figure 1. The structure of the proposed antenna.

the posts, which go through the substrate and are connected to the broadband 90° hybrid port. The dimensions of the probes and the distances between strips and annular patch affect the coupling. The fourth layer is the air layer, which can decrease the effect between the feeding network and the substrate. The feeding network is printed on the top of the top of the fifth substrate layer and the ground plane is printed on its back. The feeding network is composed of one common two-way power divider with 180° phase offset acting as the primary network and two wideband 90° hybrids acting as the secondary network. In this case, the feeding network can provide good 90° phase differences between two adjacent ports which are connected to the same wideband 90° hybrids. The structure of the feeding network is shown

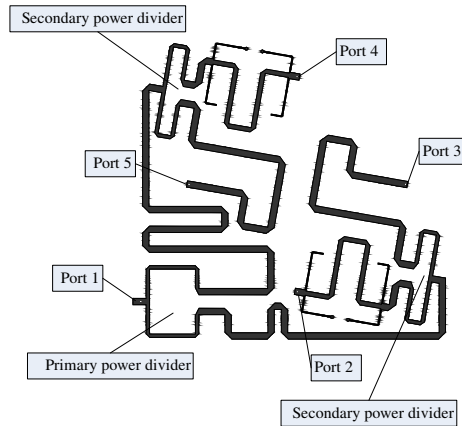


Figure 2. Layout graph of the feeding circuit.

Table 1. Key dimensions of the structure.

L	ϵ_r (all substrate layer)	d_1	d_2	d_3
100 mm	4.4	67 mm	60.8 mm	27 mm
h_1	h_2	h_3	h_4	h_5
3 mm	3 mm	6 mm	2.5 mm	1 mm

in Figure 2. Figure 3 displays the simulated (using HFSS ver.13 [22]) and measured return loss, magnitude response and phase differences of the feeding network. We observe that the magnitude variation is less than 0.5 dB and the phase shift unbalance less than 5° in the band of 1.1–1.6 GHz using the proposed feeding network. It is important for the antenna design to obtain excellent circular polarization performances.

The key dimensions of the structure are shown in Table 1.

3. RESULTS AND DISCUSSION

Figure 4 provides the graphs of the fabricated antenna. The overall size of the antenna is 100 mm \times 100 mm \times 15.5 mm. Figure 5 presents the variety of VSWR affected by the height of the third substrate (h_3) and the thickness of air gap (h_4). As can be seen in the figure, when $h_3 > 6$ mm and $h_4 > 2.5$ mm, VSWR < 2 in the whole band for GNSS. The VSWR measured using Agilent E8363B network analyzer along with the simulation data using HFSS are presented in Figure 6. It can be observed that the impedance bandwidth for VSWR < 2 is 73.7%, providing the working range of 0.9 to 1.95 GHz.

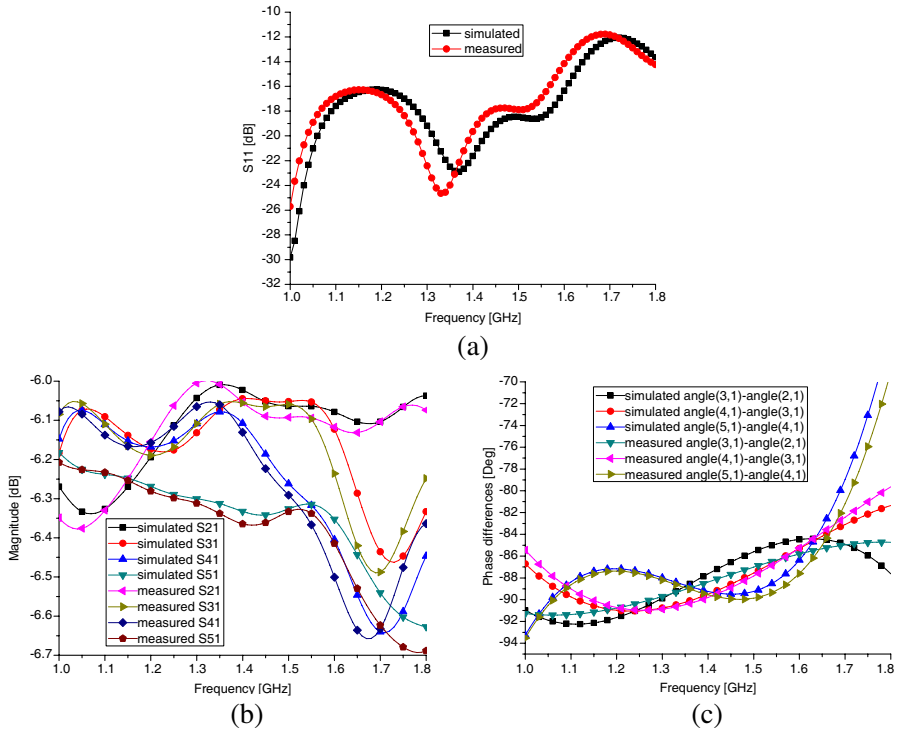


Figure 3. Simulated and measured performances of the feeding network. (a) Simulated and measured return loss of the feeding network. (b) Simulated and measured magnitude response of the feeding network. (c) Simulated and measured phase differences of the feeding network.

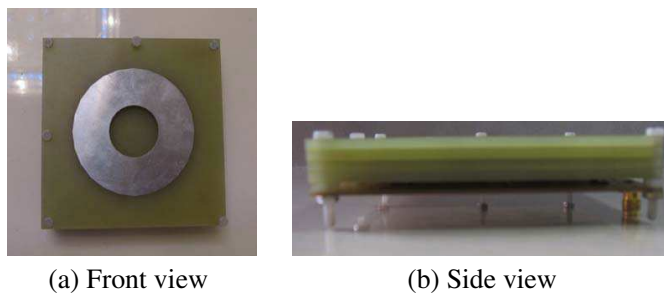


Figure 4. The photo of the proposed antenna.

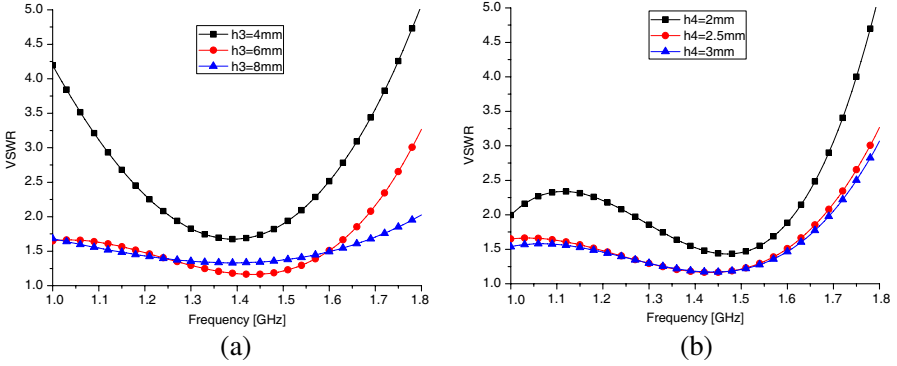


Figure 5. Simulated return loss of the proposed antenna for various h_3 and h_4 .

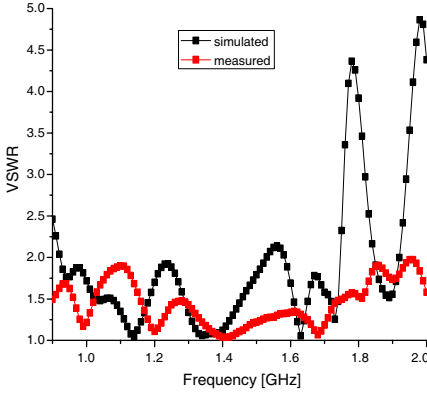


Figure 6. Simulated and measured VSWR.

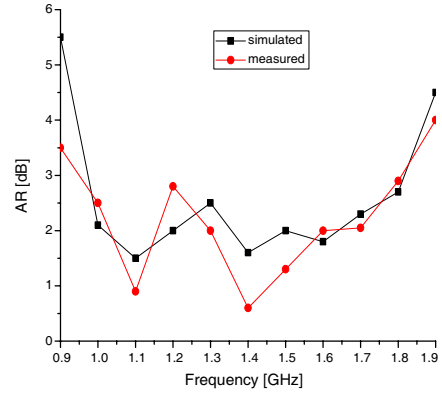
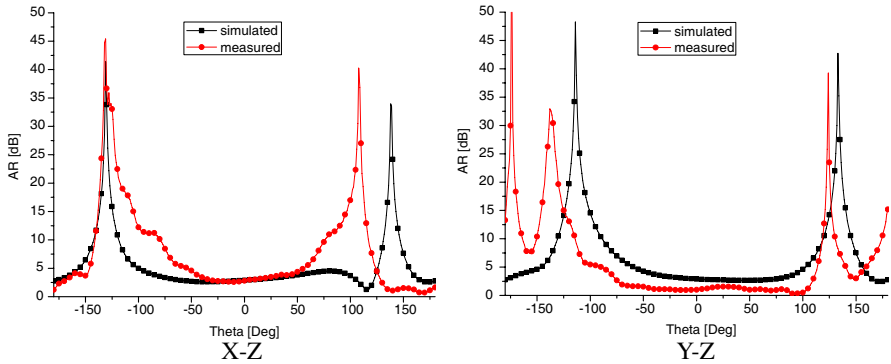
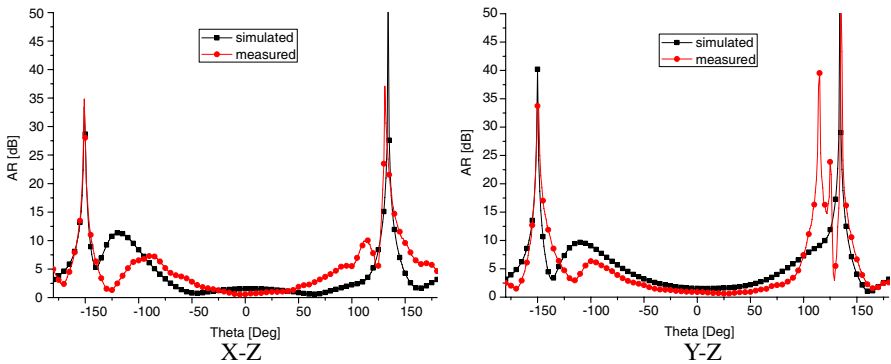


Figure 7. Simulated and measured AR.

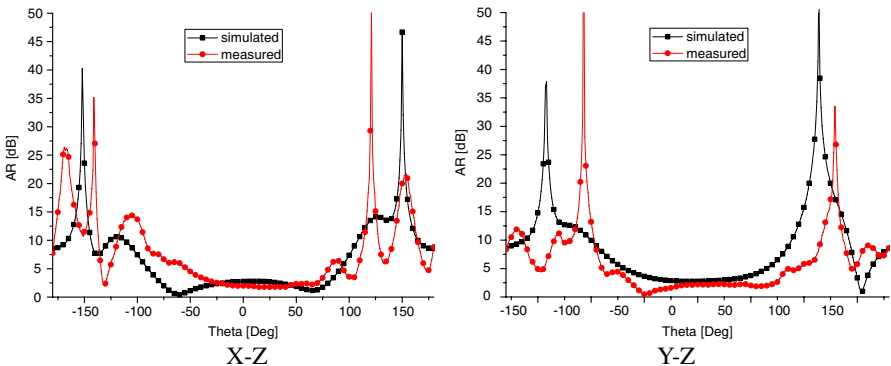
The radiation performances were measured in an anechoic chamber. Two Archimedean spiral antennas were used to measure right-hand circular polarization and left-hand circular polarization radiation, respectively. From Figure 7, the 3-dB AR bandwidth of the proposed antenna is 60.1% providing the working range of 0.96 to 1.8 GHz. It owes to applying four ports L-probes coupling feeding schemes, which enhance the AR bandwidth extremely. As can be seen in the figure, the impedance and AR bandwidths are sufficient to cover GNSS frequencies. The simulated and measured AR patterns in the X - Z and Y - Z planes at 1.2, 1.4 and 1.6 GHz are presented in Figure 8. As seen, the elevation angles for $AR < 5$ dB are -50° – 50° at X - Z



(a) Simulated and measured AR patterns at 1.2 GHz

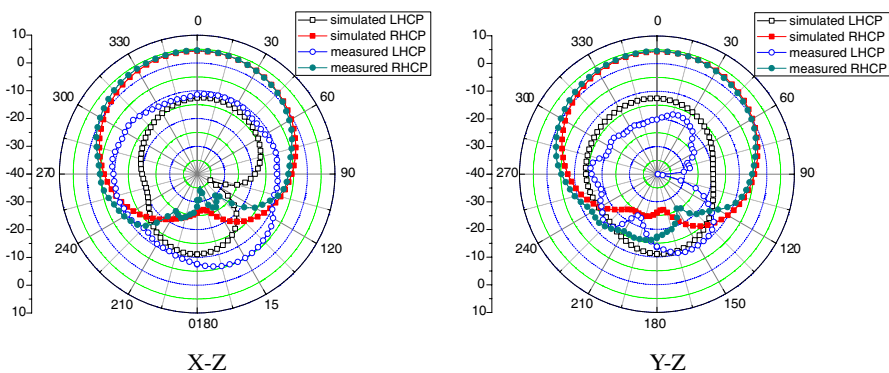


(b) Simulated and measured AR patterns at 1.4 GHz

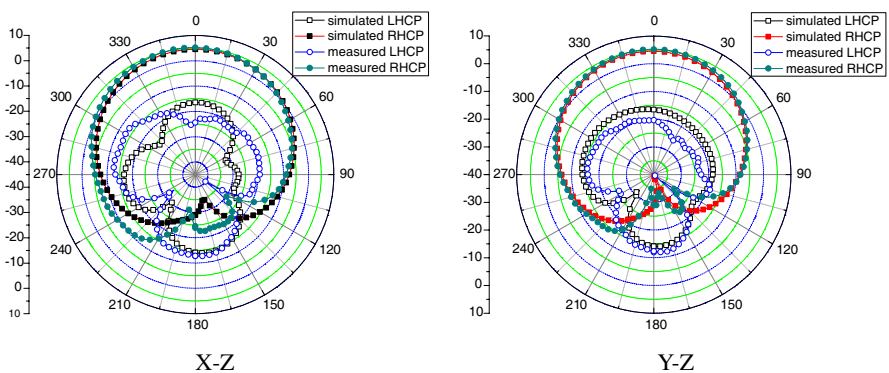


(c) Simulated and measured AR patterns at 1.6 GHz

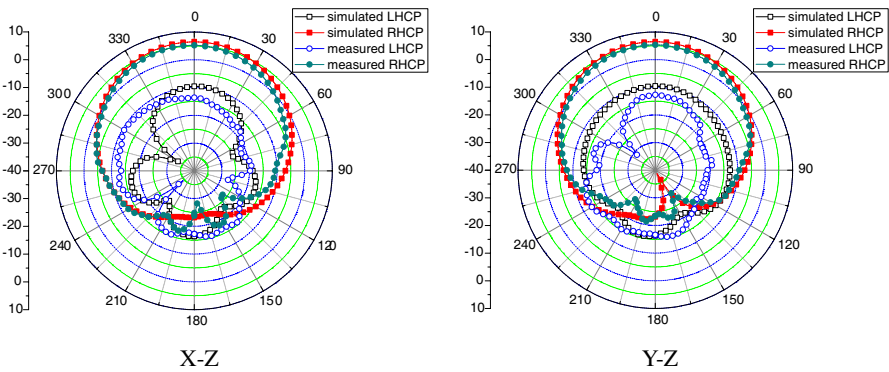
Figure 8. Simulated and measured AR patterns.



(a) Simulated and measured radiation patterns at 1.2 GHz



(b) Simulated and measured radiation patterns at 1.4 GHz



(c) Simulated and measured radiation patterns at 1.6 GHz

Figure 9. Simulated and measured radiation patterns.

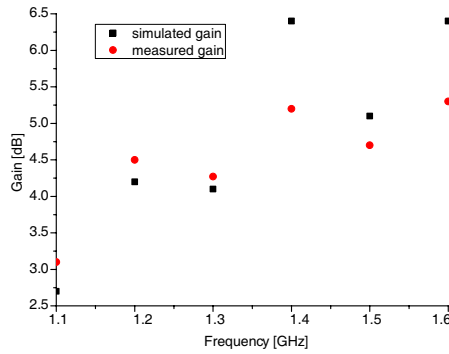


Figure 10. Simulated and measured gain of the proposed antenna.

Table 2. Axial ratio and gain characteristics at low elevation.

Literature	Elevation angles for gain > -5 dBi	Elevation angles for AR < 5 dB
7	About 20°	Not mentioned
8	About 20°	Not mentioned
9	About 20°	Not mentioned
11	About 30°	Not mentioned
12	About 30°	Not mentioned
13	About 30°	About 28°
Proposed	About 15°	About 15° expect $x-z$ plane at 1.2 GHz and $x-z$ plane at 1.6 GHz

plane and -80° – 110° at $Y-Z$ plane respectively at 1.2 GHz, -75° – 85° at $X-Z$ plane and -75° – 90° at $Y-Z$ plane respectively at 1.4 GHz, -50° – 75° at $X-Z$ plane and -85° – 85° at $Y-Z$ plane respectively at 1.6 GHz. The asymmetry of the AR patterns is mainly due to the machine and measurement errors. Figure 9 shows the simulated and measured radiation patterns in the $X-Z$ and $Y-Z$ planes at three different frequencies 1.2, 1.4 and 1.6 GHz. Broad pattern coverage and high gain at low elevation angles (more than -5 dBi at elevation angles $> 15^{\circ}$) are achieved. The excellent performances of the antenna are mainly due to the shorted annular stacked patch structure and four ports proximity-coupled probe-fed feeding mechanism. Axial ratio and gain characteristics at low elevation are better than other structures reported in the literatures [7–9, 11–13], which can be seen in Table 2. It is noted that literature [13] can achieve excellent AR

performance at low elevation angles by mounting the antenna on a cylinder housing. However, it will increase the overall size obviously. The simulated and measured RHCP gain of the antenna at different frequencies is presented in Figure 10, and it is observed that the stable gain bandwidth can be obtained for gain > 3 dBi.

4. CONCLUSION

In this paper, the results of the design for a novel compact circularly polarized shorted annular stacked patch antenna are reported. The antenna is fed by four ports feeding network composed of one common Wilkinson power divider and two broadband 90° hybrids. Using the proposed proximity-coupled probe-fed feeding scheme, the antenna exhibits an effective bandwidth of 60.1% from 0.96 to 1.8 GHz for VSWR < 2 and AR < 3 dB. Shorted annular stacked patch structure is incorporated into the antenna design. The proposed antenna not only has a compact size of $100\text{ mm} \times 100\text{ mm} \times 15.5\text{ mm}$, but also can provide stable gain bandwidth, broad beamwidth characteristics and good axial ratio at low elevation. Measured parameters show good agreement with the modeling and conform that such antennas can be successful used for GNSS applications.

REFERENCES

1. Kilgus, C., "Resonant quadrifilar helix," *IEEE Transactions on Antennas and Propagation*, Vol. 17, No. 3, 349–351, 1969.
2. Amin, M. and R. Cahill, "Compact quadrifilar helix antenna," *Electronics Letters*, Vol. 41, 672–674, 2005.
3. Huang, J. and V. Jamnejad, "A microstrip array feed for land mobile satellite reflector antennas," *IEEE Transactions on Antennas and Propagation*, Vol. 37, No. 2, 153–158, 1989.
4. Chebolu, S., S. Dey, R. Mittra, and M. Itoh, "A dual-band stacked microstrip antenna array for mobile satellite applications," *Antennas and Propagation Society International Symposium, 1995, AP-S Digest*, Vol. 1, 598–601, 1995.
5. Wu, J. Y., J. S. Row, and K. L. Wong, "A compact dual-band microstrip patch antenna suitable for DCS/GPS operations," *Microwave and Optical Technology Letters*, Vol. 29, No. 6, 410–412, 2001.
6. Guo, Y. X., L. Bian, and X. Q. Shi, "Broadband circularly polarized annular-ring microstrip antenna," *IEEE Transactions on Antennas and Propagation*, Vol. 57, No. 8, 2474–2477, 2009.

7. Zhou, Y., S. Koulouridis, G. Kizitas, and J. L. Volakis, "A novel 1.5" quadruple antenna for tri-band GPS applications," *IEEE Antennas and Wireless Propagation Letters*, Vol. 5, 224–227, 2006.
8. Zhou, Y., C. C. Chen, and J. L. Volakis, "Dual band proximity-fed stacked patch antenna for tri-band GPS applications," *IEEE Transactions on Antennas and Propagation*, Vol. 55, No. 1, 220–223, 2007.
9. Wang, Z. B., S. J. Fang, S. Q. Fu, and S. W. Lu, "Dual-band probe-fed stacked patch antenna for GNSS applications," *IEEE Antennas and Wireless Propagation Letters*, Vol. 8, 100–103, 2009.
10. Pimenta, M. S., F. Ferrero, R. Staraj, and J. M. Ribero, "Low-profile circularly polarized GNSS antenna," *Microwave and Optical Technology Letters*, Vol. 54, No. 12, 2811–2814, 2012.
11. Ma, J. P., A. B. Kouki, and R. Landry, Jr., "Wideband circularly polarized single probe-fed patch antenna," *Microwave and Optical Technology Letters*, Vol. 54, No. 8, 1803–1808, 2012.
12. Zheng, L. and S. Gao, "Compact dual-band printed square quadrifilar helix antenna for global navigation satellite system receivers," *Microwave and Optical Technology Letters*, Vol. 53, No. 5, 993–997, 2011.
13. Moernaut, G. J. K. and G. A. E. Vandenbosch, "Concept study of a shorted annular patch antenna: Design and fabrication on a conducting cylinder," *IEEE Transactions on Antennas and Propagation*, Vol. 59, No. 1, 2097–2102, 2011.
14. Kasabegoudar, V. G. and K. J. Vinoy, "A broadband suspended microstrip antenna for circular polarization," *Progress In Electromagnetics Research*, Vol. 90, 353–368, 2009.
15. Bao, X. L. and M. J. Ammann, "Comparison of several novel annular-ring microstrip patch antennas for circular polarization," *Journal of Electromagnetic Waves and Applications*, Vol. 20, No. 11, 1427–1438, 2006.
16. Liu, W. C. and P. C. Kao, "Design of a probe-fed H-shaped microstrip antenna for circular polarization," *Journal of Electromagnetic Waves and Applications*, Vol. 21, No. 7, 857–864, 2007.
17. Chang, T. N. and J. H. Jiang, "Enhance gain and bandwidth of circularly polarized microstrip patch antenna using gap-coupled method," *Progress In Electromagnetics Research*, Vol. 96, 127–139, 2009.
18. Heidari, A. A., M. Heyrani, and M. Nakhkash, "A dual-band circularly polarized stub loaded microstrip patch antenna for GPS

- applications,” *Progress In Electromagnetics Research*, Vol. 92, 195–208, 2009.
19. Yang, S. S., K.-F. Lee, A. A. Kishk, and K.-M. Luk, “Design and study of wideband single feed circularly polarized microstrip antennas,” *Progress In Electromagnetics Research*, Vol. 80, 45–61, 2008.
 20. Wu, G.-L., W. Mu, G. Zhao, and Y.-C. Jiao, “A novel design of dual circularly polarized antenna fed by L-strip,” *Progress In Electromagnetics Research*, Vol. 79, 39–46, 2008.
 21. Yu, A., F. Yang, and A. Z. Elsherbeni, “A dual band circularly polarized ring antenna based on composite right and left handed metamaterials,” *Progress In Electromagnetics Research*, Vol. 78, 73–81, 2008.
 22. Ansoft High Frequency Structure Simulation (HFSS), ver. 13, ANSYS, Inc., Canonsburg, PA, 2011.